行政院國家科學委員會專題研究計畫　成果報告

醫學組織工程用之自身方向性排列無機奈米磷灰石/有機基質奈米複合材料製程與特性研究

計畫類別：個別型計畫
計畫編號：NSC92-2216-E-009-025-
執行期間：92 年 08 月 01 日至 93 年 07 月 31 日
執行單位：國立交通大學材料科學與工程學系

計畫主持人：陳三元

報告類型：精簡報告
報告附件：出席國際會議研究心得報告及發表論文
處理方式：本計畫可公開查詢

中　華　民　國 93 年 9 月 14 日

醫學組織工程用之自身方向性排列無機奈米磷灰石/有機基質奈米複合材料製程與特性研究(I)

Synthesis and characterization of nanoapatite-based nanocomposites with controlled aspect ratios for scaffold application

奈米缺鈣磷灰石合成與奈米複合材料製程與特性研究
計畫編號：NSC92-2216-E-009-025
執行時間：92/08/01～93/07/31

主持人：陳三元 教授　　交通大學材料科學與工程學系

中文摘要

無機奈米磷灰石，是一種生物相容性及可降解的無機奈米材料，本研究主要是在探討無機奈米磷灰石粉體的合成與成長機制及形態發展，研究發現不僅在常溫即可合成 β-TCP phase。而且可經由 PAA couple agent 的添加與溶液 pH(9-11)的改變，來控制 CDHA 的核凝與成長反應，發展出直徑約 5-10 nm 而長度約 20-80 nm 等具有不同長寬比(Aspect ratio)的無機奈米磷灰石(CDHA)粉末，可用於強化生化有機基材。並且研究中發現，在奈米磷灰石(CDHA)粉體之表面包覆一層 PAA 有機高分子—而形成 core-shell 結構，顯示 PAA 的添加對於這些鈣—磷無機物之成長的形態及尺度大小扮演一個重要的角色。因此在未來可以利用表面改質，從製程的研究，以發展具有特殊方向性排列之機械強化的仿支架奈米生化複合材料。

關鍵字： 奈米缺鈣磷灰石、奈米複合材料、微結構形態、方向性成長

Abstract

Calcium-deficient apatitic (cd-HA) crystals with core-shell nanostructure of needle-like shape of 5-10 nm in diameter and 20-80 nm in length were prepared via an in-situ formation in the presence of polyacrylic acid (PAA) under aqueous solution of different pH values ranging from 9 to 11. Nanostructure of the resulting crystals was investigated, showing a core-shell configuration with a thin layer of PAA shell of about 1 nm thick. Aspect ratio (AR) of the needlelike composite was found to depend on the concentration of the PAA and solution pH. At lower solution pH, crystal growth was inhibited, i.e., leading to a decreased AR, with increase of PAA concentration, whilst an increased AR was detected at higher solution pH, suggesting a preferential growth of the cd-HA nano-crystals. Mechanism of such preferential growth was tentatively proposed and is suggested to correlate with PAA adsorption along the long axis of the needlelike nanoparticles.

Keywords: Calcium-deficient apatitic, nanocomposite,；microstructure morphology；preferential growth

1. Introduction

Synthetic calcium phosphate compounds, particularly in the composition of tricalcium phosphate (Ca/P = 1.5) and calcium hydroxyapatite (Ca/P = 1.67), has long been received a great deal of attention as prime candidates for a number of biomedical applications such as orthopedics and dentistry, simply because they exhibit considerably improved biological affinity and activity, compared to currently existing synthetic materials, to surrounding host tissues when implanted. Furthermore, both compositions are chemically and structurally similar to the mineral constituent of human hard tissue. However, bone mineral (natural biocrystal) has

essentially a calcium-deficient apatitic structure with a Ca/P ratio of about 1.5, which strictly speaking, is chemically compositionally similar to tricalcium phosphates, $Ca_3(PO_4)_2$, (Ca/P = 1.5) and structurally similar to stoichiometric hydroxyapatite, $Ca_{10}(PO_4)_6(OH)_2$, (Ca/P = 1.67).

Natural biocrystals exhibit nanostructured with a needlelike or rodlike shape well arranged within the polymeric matrix, e.g., collagen, to form natural bone. Most critically, biocrystals exhibit excellent metabolic activity even when subject to subtle environmental changes, compared to those synthetic biocrystals [1-3]. It is still not fully understood the mutual interaction between natural biocrystal and surrounding physiological environment, but the natural biocrystals do provide a more dynamic response to environment than that of synthetic materials. One of the reasons may be arisen from the poorly-crystalline and nanostructured feature of the natural biocrystals that formed at ambient environment. Both structural characters give considerable dynamics to these "biocrystals" in terms of enhanced contact areas and degradation-formation (or re-deposition) property to the environment, which is essentially a structurally-induced chemical and biological response. However, this is seldom seen in synthetic biocrystals, where the nanostructured and low-crystalline characters can be loss after thermal consolidation to form solid entity. This is also the reason for many biomaterials researchers nowadays who employed so-called biomimetic method to form nanostructured apatitic crystals [1, 4-6].

Recently, it is more advanced to use different methodologies to form nano-crystal-contained composites (or termed nanocomposites) at ambient temperature, for a variety of biomedical applications [7-9]. Among those existing methodologies, in-situ formation of the nanocomposites by forming the nano-apatite crystals in the presence of polymers is one of most attractive routes, since it avoids extensive particle agglomeration if a mechanical mixing between nanopowder and selected polymer was adapted. Kato et al. [7] studied a series of nano-crystalline hydroxyapatite/polymer composites via an in-situ synthesis method, they found that the crystallization of the hydroxyapatite was retarded in the presence of ionized polymers employed and showed a concentration-dependent manner, which we found similar behavior in our study. As an integral part of the whole project to be elucidated in this communication, we focus on the in-situ synthesis of composite-type nano-grade crystals, instead of pure inorganic crystals as frequently reported, with controlled morphology and here the calcium phosphate materials with a Ca/P ratio of 1.5 was employed instead of stoichiometric hydroxyapatite, since it represents closer chemical resemblance to natural biocrystals than stoichiometric apatite.

2. Experimental Procedure

2.1 Sample preparation

The starting materials used in this investigation were analytical-grade $(CH_3COO)_2Ca{\cdot}xH_2O$ (99%, Aldrich Chemical company, Inc., USA) which is used as the Ca source, and H_3PO_4 (85%, Riedel-deHaen, Seelze, Germany) as the P source. After dissolving 0.015 mole $(CH_3COO)_2Ca{\cdot}xH_2O$ in deionized water, poly (acrylic acid) (Mw 450000) (PAA, Aldrich Chemical company, Inc., USA) was added to the solution and adjusted the solution to different pH values, in this investigation pH is controlled over the range of 9, 10 and 11 using 5M NaOH solution. Phosphoric acid (0.01 mole) was then dropped into the above solution and at the same time, the sodium hydroxide solution was used to keep the solution at pre-determined pH level throughout the entire synthesis procedure. All the reaction is processed at room temperature (25^oC) and following an ageing time period of 16h. After filtering and washing with deionized water several times, white precipitated powder was finally obtained after drying overnight at 80°C, having a Ca/P ratio of 1.5 as pre-determined,

using atomic absorption spectroscopy analysis.

2.2 Phase analysis

X-ray diffractometry (M18XHF, MAC Science, Tokyo, Japan) was used for identifying the crystalline phase of the synthesized compounds at a 4° 2θ/min from 20 to 60°.

2.3 Fourier Transform Infrared Ray (FT-IR) Spectroscopy

Fourier transform Infrared ray (FT-IR) spectra were performed using KBr pellets (2 mg per 300 mg KBr) on a spectrometer (Model 580, Perkin-Elmer) with a resolution of 4.00 cm^{-1}. Infrared spectra were recorded in the range of 4000-400 cm^{-1} to evaluate the molecular structure and phase clarification of the resulting powders.

2.4 Transmission Electron Microscopy Analysis

The powder sample was ultrasonically dispersed in ethanol to form very dilute suspensions and then dropped a few droplets on copper grids with carbon film coated. Microstructure observations were performed in Philips Tecnai 20 (Holland, The Nertherlands) microscope operating at 200 keV.

3. Results and Discussion

3.1. Phase Identification

The use of macromolecules as templating agent to manipulate the growth of inorganic crystals has been realized in many biological systems. In the presence of biological macromolecules (such as collagen), the nucleation and growth of nanocrystalline apatite to form highly organized bone minerals is one of the most fascinating processes in nature. Likewise, in the past in forming nanocrystalline apatite, some attention was paid to the control synthesis of apatitic crystals via physical approaches such as temperature control, aging, etc. [10-13].

A number of earlier studies indicated that poly(acrylic acid), PAA, is an inhibitor for the crystallization of apatitic crystals [7,14-15]. Interaction between ionized PAA anions and Ca cations to form PAA^- - Ca^{++} intermediate compound delays the desired interaction of P and Ca ions in forming the apatite. In this study, the synthetic precipitate powders with a Ca/P ratio of 1.5 (chemically determined) show a poorly-crystalline apatitic identification, as shown in Fig. 1(a) and (b), for pH 9 and 11, respectively, regardless of the solution pH range of study. A major characteristic diffraction pattern is as follows: a peak at 2 of ~ 26^o and a broad one at ~32^o for the powders obtained. These peaks are almost identical to those in stoichiometric microcrystalline hydroxyapatite (sm-HA), but with much poorer diffraction resolution compared to sm-HA, particularly at 2 ~32^o. This suggests the synthetic powders are apatite-like crystals, and hence are considered to be calcium-deficient HA (CDHA). However, upon close inspection of the diffraction intensity of the major characteristic peak at 32^o, it is evidenced that the crystallinity of the resulting powders becomes even poorer with increasing PAA concentration for pH10 and pH11 cases, while the crystallinity remains almost unchanged (i.e., similar diffraction intensity) for solution at pH = 9.

Molecular arrangement of the precipitate powders can be further identified through the use of Fourier Transform Infrared Ray (FT-IR) analysis, where as selectively shown in Fig. 2 is the IR spectra of the powders prepared in the presence of 0.05 wt% PAA at different solution pH. It is clearly showed the presence of two characteristic $_4PO_4$ bands at around 563 cm^{-1} and 600 cm^{-1}, and $_3PO_4$ band in the range of 1100-1000 cm^{-1} in all the cases, which are characteristic molecular structure in the apatitic lattice. Some carbonate groups were detected at ~1400 cm^{-1}, and one broad absorption bands at ~3500 cm^{-1}, designated as hydroxyl groups.
These IR spectra further confirm the apatitic structure of the powders prepared and both chemically and structurally identified to be CDHA. The bands in the range of 1750 cm^{-1} –

1450 cm^{-1} are assigned to the characteristic absorption peaks of PAA molecules. This observation indicates that the powders prepared in this study were virtually a mixture of inorganic CDHA crystals and organic PAA.

The decrease in diffraction intensity with increasing PAA concentration agrees with previous observations, where an inhibiting effect of PAA molecules on crystallization of apatite can be well explained [7,15]. Increase in PAA concentration indicates increased amount of dissociated PAA anions, i.e., carboxylic ion $(COO)^-$, in the aqueous solution;

$$PAA \leftrightarrow PAA(COO)^- + H^+ \quad (1)$$

A further association of $PAA(COO)^-$ and Ca^{++} results in a complex compound which can be of the simplified form;

$$PAA(COO)^- + Ca^{++} \leftrightarrow PAA(COO)Ca(COO)PAA \quad (2)$$

Or most likely, as a form of ionic species proposed in Reaction (8-3), since the solutions remain clear after Ca ions were mixed with PAA polymer solution and no sign of precipitate or visible colloidal complex can be optically detected;

$$PAA(COO)^- + Ca^{++} \leftrightarrow PAA(COO)Ca^+ \quad (3)$$

A further dissociation of Reaction (8-2) is possible, which gives anionic species as the one described in Reaction (8-3);

$$PAA(COO)Ca(COO)PAA \leftrightarrow PAA(COO)^- + PAA(COO)Ca^+ \quad (4)$$

According to previous investigation [7], a Ca - PAA(COO) complex formed rapidly in aqueous solution which further inhibits desired reaction between available Ca ions and phosphate ions to form crystalline apatite. This mechanism not only suppresses the formation of crystalline apatite, i.e., inhibition of nucleation, but also retards the growth of the apatitic crystals, which will be further elucidated in forthcoming analysis. For solution at pH = 9, the diffraction intensity of the characteristic peaks remains unchanged irrespective of the PAA concentration, and in a qualitative comparison, the characteristic peaks are generally stronger in intensity for solution pH 10 and 11 than at pH = 9. This indicates a gradually degraded crystallinity of the cd-HA developed or resulting crystallites getting smaller in dimension at pH 9.

One possible explanation on those differences in structural development between pH 9 and those > pH10 is due to degree of dissociation of the PAA. According to Reaction (1), lower [OH] concentration, having 1 and 2 orders of magnitude lower than those at pH 10 and pH 11, respectively, when PAA was dissolved in solution at pH 9. This enables the movement of Reaction (1) toward left-side, rather than right-side, resulting in lower concentration of ionized $PAA(COO)^-$ species in the solution. Lower concentration of the $PAA(COO)^-$ anions renders the Ca ions in the solution that chemically interacted with PAA(COO)- ions to form intermediate complex becoming less in quantity at pH 9 than at pH 10 and pH 11. This is further evidenced by Bao et al. [16], who indicated a complete dissociation of PAA when solution pH is greater than 10.

By employing the growth inhibition effect of the PAA, this investigation has three-fold purpose; (1) to manipulate the growth of CDHA crystals to form nanometric particles of control morphology (2) to develop CDHA with relatively poor crystallinity, and (3) to develop CDHA – PAA composite-type nanocrystals for subsequent synthesis of nanocomposites and this will be elucidated elsewhere.

3.2. Powder Morphology

Figure 3 shows the morphology of the precipitated CDHA powders at different pH levels. The precipitated powders show similar needlelike shape regardless of solution pH and the amount of PAA used. This suggests both the hydroxyl groups and PAA ions having little influence on the morphological development of the CDHA crystals. However, according to literature, nucleation of the HA crystallites and their crystallization will be strongly inhibited in the presence of PAA ions [7]. However, in this investigation, attention is placed more on the

growth of CDHA crystals and the experimental observation did show a strong influence on CDHA crystal growth. Figures 4 a-c show the dimensional length of the CDHA crystals in both radial (diameter) and axial (length) directions measured in terms of different PAA concentrations at pH 9, 10, and 11, respectively, which has dimensions of 5 - 10 nm in diameter and 20 - 80 nm in length. A rapid decrease in the length of the needlelike nano-crystals appears in both axial and radial directions when a small amount of PAA ions was present in the solution. The reduction in dimensional length in both directions is similar, which has about 40-50% for PAA concentration from 0% to 0.01 wt%. This observation gives a direct evidence of the influence of the PAA on the crystal growth of the CDHA nano-crystals. Further increase in PAA causes a further reduction of the resulting CDHA crystals; however, in some cases, which are not clearly understood at present, nano-crystals. Further increase in PAA causes a further reduction of the resulting CDHA for solutions at higher solution pH, an increase of the length in both directions was detected when the PAA concentration is in the range of 0.05-0.1 wt%. As a general trend on the crystal growth, PAA does inhibit the growth of the CDHA nano-crystals in a considerable extent over the PAA concentration and pH range of study.

The inhibition effect can be resulting from the adsorption of the dissociated or un-dissociated PAA ions onto the surface of CDHA crystals, although the natures of the adsorption (for both dissociated and un-dissociated groups) are unclear at present. This also indicates the cd-HA crystals being isolated by surrounding PAA molecules once the nuclei were formed in the solution. This isolation considerably suppresses subsequent crystal growth.

The aspect ratio (AR = length/diameter) of the resulting needlelike nano-crystallites is presented in Fig. 5 with respect to the concentration of PAA at different solution pH. The standard deviation of the AR obtained is between 0.5 and 1.6 for all the measurements, which is within the size of the symbols employed in each curve. For pH 9, the AR is decreased gradually from 10 to 4 with increasing PAA, for pH 10, the variation of AR is not considerable but remained in the range of 5-7; however, for pH 11, an increase in the AR from 5 to 9 is appeared. This suggests that the growing mechanism of the CDHA nano-crystals not only being suppressed, but being preferentially oriented in the presence of PAA molecules. This point, to our knowledge, has not been reported in the literature and it has a profound implication to the control growth of the CDHA crystals that have a number of biomedical and engineering uses.

The mechanism of such a preferential growth of the CDHA needlelike nanocrystals is not fully understood. However, since the only variable in this comparison is solution pH, it is possible to account for this phenomenon in terms of the dissociation degree of PAA molecules as a result of hydroxyl concentration, i.e. [OH], in the solution, as aforementioned in Reaction (1). Based on the observed crystal growth of the CDHA, it is reasonable to assume that the dissociated $PAA(COO)^-$ ions are preferably adsorbed onto the surface perpendicular to the radial direction of the cd-HA crystals, that is, the *a-axis* of the lattice (schematic draw in Fig. 6), which, for instance, has a surface area at least 10 times higher than that of the area perpendicular to the axial direction of the needle for needles with an aspect ratio above 5. The highly-negatively-charged PAA ions possibly strongly interact with the surface Ca ions to form the intermediate compound (Reaction 2) on the needle surface. This chelating compound causes a retardation of crystal growth more in the radial direction than in the axial direction (*c-axis* of the lattice) of the nano-needle, leading to higher AR of the resulting crystals. Accordingly, this can be the case of pH = 11, which, according to Reaction (1), should produce more dissociated PAA ions, or

preferably, more dissociated carboxyl groups in the PAA macromolecules, giving stronger interaction with the surface.

On the other hand, at pH 9 the population of the dissociated carboxyl groups may be reduced by 1-2 orders in concentration compared to that at pH 10 and pH 11, respectively. This may cause the macromolecular PAA ions less negatively charged than that at higher solution pH. Then, lesser extent of interaction to the surface Ca ions on the *a-axis* of the lattice can be expected, where the potent of crystal growth in the radial direction is then not considerably suppressed, resulting in a reduced AR. It is also found from the experimental observation that at pH 10, the growth of the CDHA nano-crystals is not considerably different, resulting in a similar level of AR of the final crystals, irrespective of PAA concentration. Therefore, it is more interesting to realize that a controlled morphological development of the needlelike CDHA nano-crystals can be easily and precisely manipulated through the control of solution pH and corresponding concentration of ionized PAA macromolecules. Nanocomposites with distinctly different physical properties can be manipulated based on the needlelike nano-crystals with controlled AR and orientation, which will be further elucidated elsewhere.

3.3. Nanostructured Analysis

Under TEM analysis, we found that the CDHA is susceptible to degrade under electronic beam bombardment, which is likely due to conversion of hydrogen ions into hydrogen gas. This disappearance of the hydrogen due to electronic beam bombardment may lead to such a transformation or shape change. In this study, the shape change was only observed in some conditions with PAA amount less than 0.1 wt% in pH9. On the other hand, when the addition of the PAA was more than 0.1 wt%, the shape of the CDHA crystal remains unchanged under TEM electronic beam bombardment.

High-resolution TEM showed that an axial zone in some needlelike particles can be clearly observed in Fig. 7. A white line dissecting the cd-HA nano-crystals in the center and through their long axis was merely observed in this study. The central line was seen predominantly in long needlelike crystallites parallel to (100) CDHA lattice fringes, having a width of 0.82 nm, and was bounded by dark Fresnel-like fringes. The central defect line of the CDHA nano-crystals is occasionally observed in this work; however, the forming mechanism has not yet been fully understood at present. Nelson *et al*. [17] considered that the central planar defect could be the initial nucleus during biological apatite precipitation and act as a template onto later apatite precipitates.

Moreover, a thin layer of amorphous material surrounding the needle was observed and has an average thickness of about 1 nm along the surface of the CDHA needle crystals. This layer is believed to be the PAA, which encapsulates the nano-crystals by either physical or chemical interaction, or both combinations during synthesis, to form a core-shell nanostructured composite.

3.4. Thermal Analysis

While subjecting to thermal treatment, the filtered and thoroughly washed nano-powders showed similar weight loss behavior for solutions with different PAA concentrations, as representatively depicted for the case at pH 9 in Fig. 8 (similar weight loss behavior was also observable for the cases at pH 10 and pH 11). In general, the residual PAA on the cd-HA nano-powder showed a two-step weight loss; one with a slow change in the weight loss curve in the temperature range from 25 to about 360^{o}C, corresponding to the vaporization of residual water and possibly desorption of some weakly-adsorbed PAA molecules. Following the slow change in weight loss, a steeper change in the weight loss curve appears until about 500^{o}C, which corresponds the thermal decomposition of PAA.

However, there seems no appreciable change

in the weight loss curve above 500°C till 1000°C, except the one with 0.3% PAA where weight loss of 6.6% was detected. This weight loss region for the case of 0.3% PAA can be further divided into two stages; 500-800°C, having 5.2% loss, and 800-1000°C, 1.4% loss. Those high-temperature weight loss regions can be attributed to the pyrolytic cleavage of carboxylate- CDHA bonds at interface and the loss of water as a result of thermal decomposition of CDHA, to form tricalcium phosphate (TCP), and has been confirmed by XRD analysis (not shown). Thermal decomposition at elevated temperature results in water elimination and this can generally be expressed by;

$$Ca_{10-x}(PO_4)_{6-x}(HPO_4)_x(OH)_{2-x} \rightarrow Ca_{10}(PO_4)_6(OH)_2 + Ca_3(PO_4)_2 + xH_2O \quad (5)$$

where the calcium-deficient hydroxyapatite is thermally transformed into tricalcium phosphate (TCP) or a mixture of HA and TCP. In this investigation, the possible reaction can then be proposed as a simplified form, where x = 1;

$$Ca_9(PO_4)_5(HPO_4)(OH) \rightarrow 3\ Ca_3(PO_4)_2 + H_2O \quad (6)$$

The elimination of water is about 2% from Reaction (6), which is slightly higher than the measured value for the case of 0.3% PAA, suggesting partial decomposition of the CDHA nanocrystals, resulting in a mixture of CDHA and TCP.

However, closer inspection of the weight loss curve shown in Fig. 8, a similar but weak weight loss peak was recorded at temperatures higher than about 700°C for PAA of 0.05 and 0.1 wt%, although the change in weight loss behavior is getting weaker with decreasing PAA. The XRD spectra did not show detectable phase change from cd-HA to TCP for lower PAA concentrations. However, we believed there should have some phase transformation, as detected in the case of 0.3wt% PAA, but may be far below the resolution limit of the XRD.

Figure 9 a-c show resulting weight loss estimated at temperatures range of 25 - 500°C for pH 9, 10, and 11, respectively. The weight loss at this temperature region is attributed to those volatile components, such as adsorbed and absorbed water molecules, and decomposition of the PAA molecules. Based on Figs. 8 and 9, it appears that the residual PAA deposited on the CDHA nano-powder is increased with PAA concentration.

The increase in the weight loss at higher PAA concentration can be due to an increased adsorption amount on the surface of the nano-particles, which in certain case, is further associated with an increased surface area as a result of decrease in particle size with increasing PAA. This should be more pronounced for the case at pH 9, since a continuing decrease in particle size (in both axial and radical directions) was detected with increasing PAA concentration. However, for the cases at pH 10 and pH 11, it is reasonable to assume that the total surface area that is available for PAA molecules to adsorb can be either remained similar (pH 10) because of the change in particle dimension is relatively small or in some case, even decreased (pH 11) because of increasing particle dimensions in the PAA between 0.01 to 0.3 wt% under this investigation. This can further be evidenced that a saturated adsorption was detected at about 30% when the PAA is controlled at a concentration $\geq$ 0.1 wt% for pH 11, whilst a similar behavior, i.e., approaching to a saturated adsorption, as depicted at pH 11, was also detected at PAA > 0.2 wt% for pH 10. The adsorption is continuously increased up to 32 % by weight when PAA is increased up to 0.3% in solution at pH 9, where the "saturated" adsorption seems approaching when PAA is approaching 0.3% in the solution.

Based on above findings, it shows that a "saturated" adsorption of the anionic PAA onto the CDHA can be obtained with a critical PAA concentration relying on solution pH; more specifically, to reach saturation adsorption, the minimum amount of the PAA in the solution is moving from lower (~ 0.1%) to higher content (> 0.3%) when the solution chemistry is moving

from higher (11) to lower pH (9) level. This indicates the adsorption behavior is a strong function of solution pH, and accordingly, is essentially a complicated function of the surface chemistry of the nano-particles, degree of ionization of the PAA molecules, and charge state on particle surface, as previously being reported [16,18]. The increased amount of PAA adsorbed at pH 9, e.g., 2% (= 32%-30%), can be attributed to the increase in the surface area as a result of size reduction of the CDHA nano-particles prepared at pH 9 in a given quantity of the starting precursor.

4. Concluding Remarks

In-situ forming of needlelike calcium-deficient hydroxyapatite (CDHA) nanocrystals with a core-shell composite structure was synthesized in the presence of high-molecular-weight polyacrylic acid (PAA). The structural development of the core-shell CDHA nanocomposites was manipulated over an aspect ratio from 4 to 10. Experimental results indicate solution pH being a predominant factor for the preferential growth, thus the aspect ratios, of the CDHA nanocrystalline composite during microstructural evolution. The mechanism of the preferential growth was proposed and is believed to strongly relate to the preferred adsorption of the PAA anions along the surface of developing CDHA nanocrystals. It is more instructive of utilizing the needlelike CDHA nanocrystals to form nanocomposites of different shapes for a number of biomedical and engineering applications.

Acknowledgement

The authors gratefully acknowledge the National Science Council of Taiwan for its financial support through Contract No. NSC-91-2216-E-009-025.

References

[1] Kim HM, Kim Y, Park SJ, Rey C, Lee HM, Gimcher MJ, Ko JS. Biomaterials 2000; 21: 1129.
[2] Legeros RZ. Adv Dent Res 1988;2:164.
[3] Hench LL. Bioceramics: from concept to clinic. J Amer Ceram Soc 1991;74: 1487.
[4] Liu DM, Yang Q, Troczynski T. J Mater Sci:Mater in Med 2002; 13:965.
[5] Wen HB, De Wijn JR, Cui FZ, De Groot K. J.Biomed Mater. Res 1998;41:227.
[6] Lin S, Campbell AA. US Patent #5 958 430, 1999.
[7] Kato K, Eika Y, Ikada Y., J. Mater Sci: Mater in Med 1997;32 5533.
[8] Yamaguchi, Tokuchi K, Fukuzaki H, Koyama Y, Takakuda K, Monma H, Tanaka J., J. Biomed Mater Res 2001;50:20.
[9] Liu Q, De Wijn JR, Van Blitterswijk CA. Biomaterials 1997;18: 1263.
[10] Ahn ES, Gleason NJ, Nakahira A, Ying JY. Nano Letters 2001;1[3]:149.
[11] Akao M, Aoki H, Kato K., J. Mater Sci 1981;16:809.
[12] Jarcho M, Bolen CH, Thomas MB, Bobick J, Kat JF, Doremus RH., J. Mater. Sci 1976;11:2027.
[13] Fang Y, Agrawal DK, Roy DM. , Mater Letters 1995;23:147.
[14] Kamitahara M, Kawashita M, Kokubo T, Nakamura T., Biomaterials 2001;22: 3191.
[15] Amjad Z.,Phosphorus Res Bull 1995;5:1.
[16] Bao Y, Senos AMS, Almeida M, Gauckler LJ., J. Mater Sci: Mater in Med 2002;13: 639.
[17] Nelson DGA, Wood GJ, Barry JC, FeatherstoneJDB.,Ultramicroscopy, 1986 ; 19:253-66.
[18] Borozhkina EI, Dorozhkin SV., Chem Mater 2002;14:4267-72.

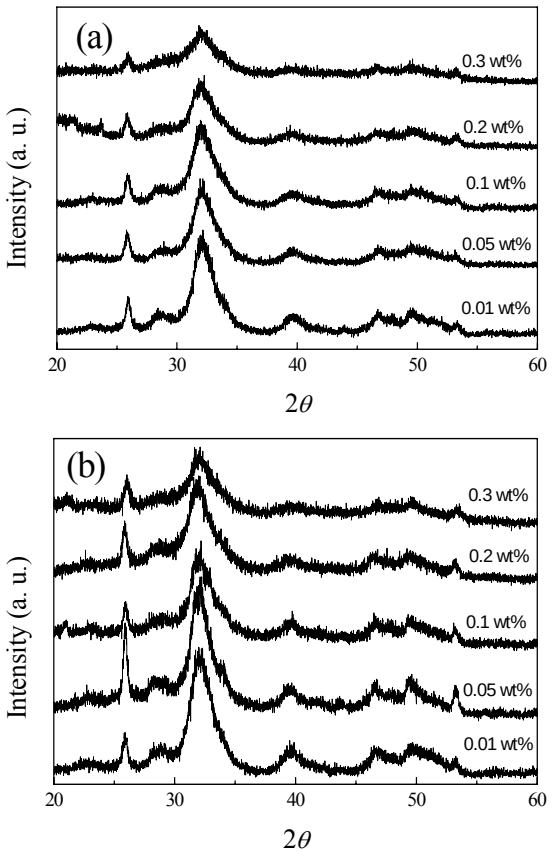

Fig. 1 XRD patterns of synthetic precipitate powders with different PAA concentration at (a) pH9, and (b) pH11

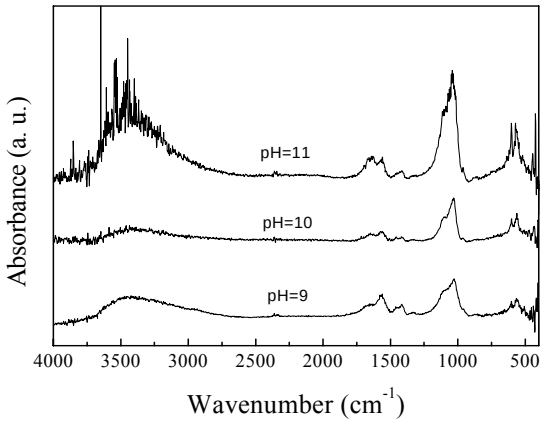

Fig. 2. FT-IR spectra of the synthetic precipitate powders prepared in the presence of 0.05 wt% PAA at different

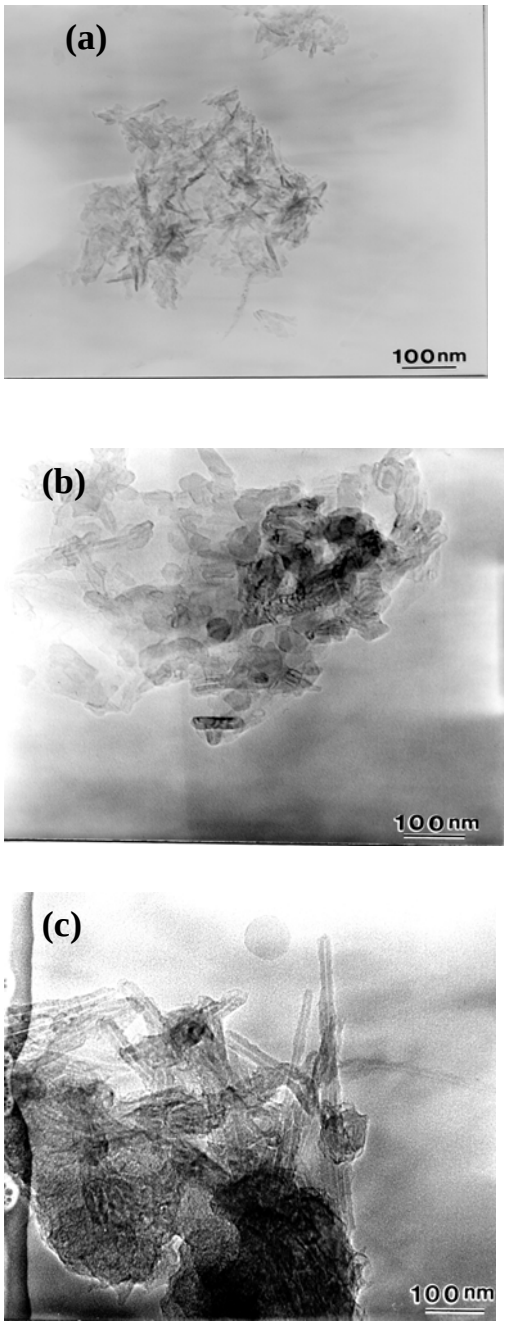

Fig. 3. Morphology of precipitated CDHA powders at different solution pH, (a) pH9, (b) pH10 and (c) pH11.

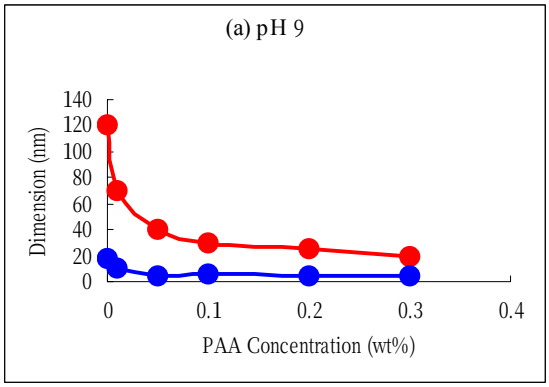

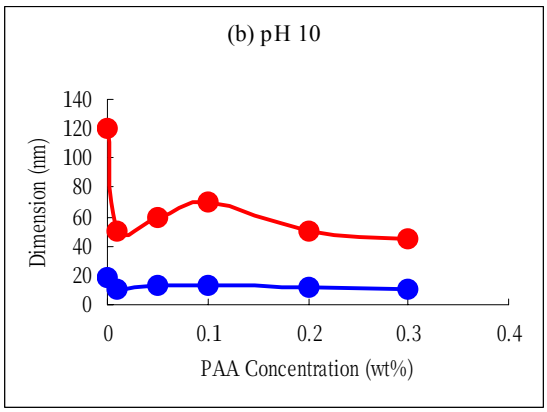

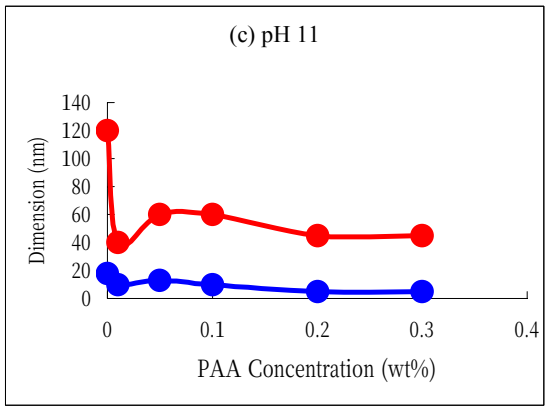

Fig. 4. Dimensional length of CDHA crystals in both radial and axial directions vs. different PAA concentrations at different solution pH, (a) pH9, (b) pH10 and (c) pH11

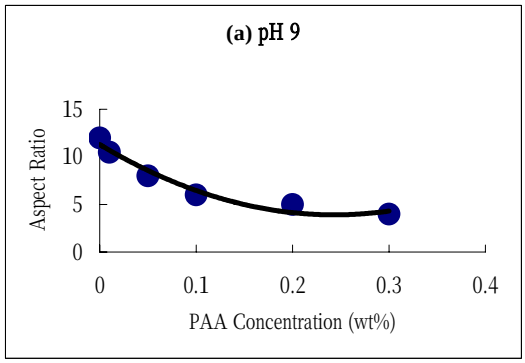

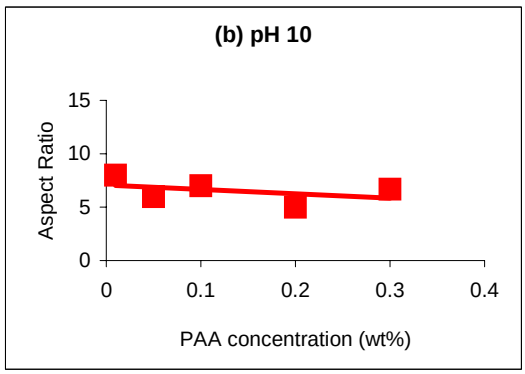

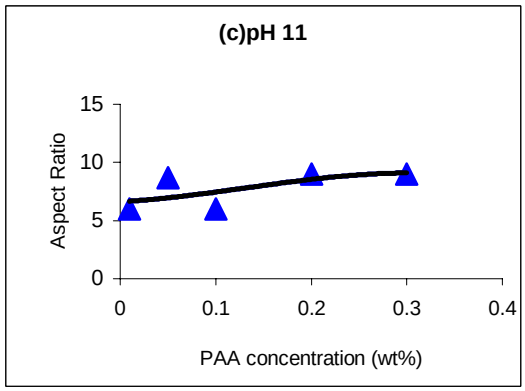

Fig. 5. The aspect ratio of the resulting needlelike nano-crystallites with repect to PAA concentration at different solution pH, (a) pH9, (b) pH10 and (c) pH11

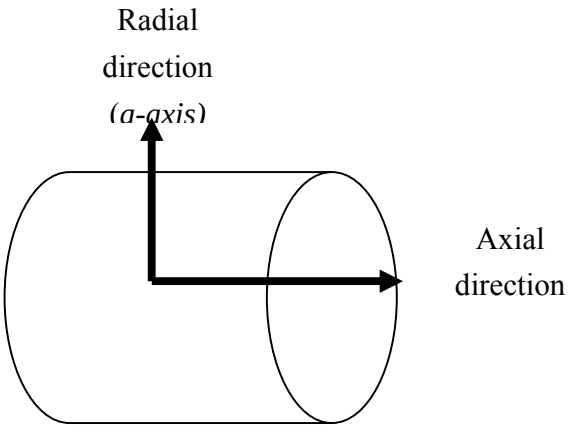

Fig. 6 Schematic illustrations of the CDHA crystals in both a-axis and c-axis of the needlelike crystal.

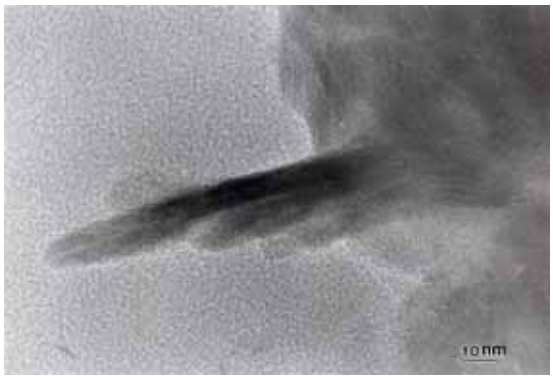

Fig. 7 High-resolution lattice fringes in the needlelike particle of CDHA crystal.

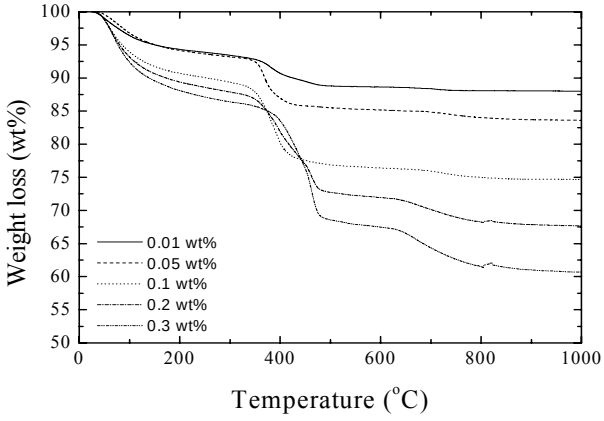

Fig. 8 Weight loss behavior of synthetic recipitate powders prepared in solution pH9 with different PAA concentrations.

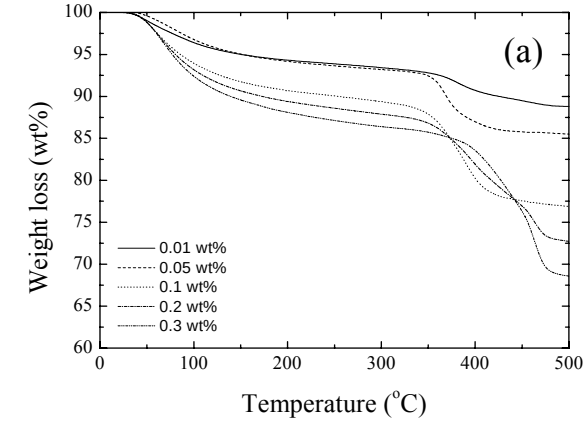

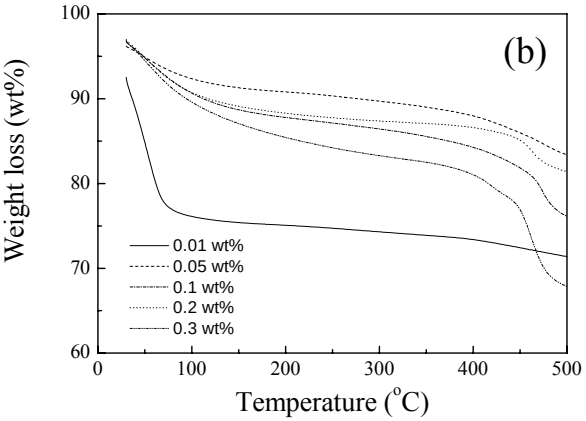

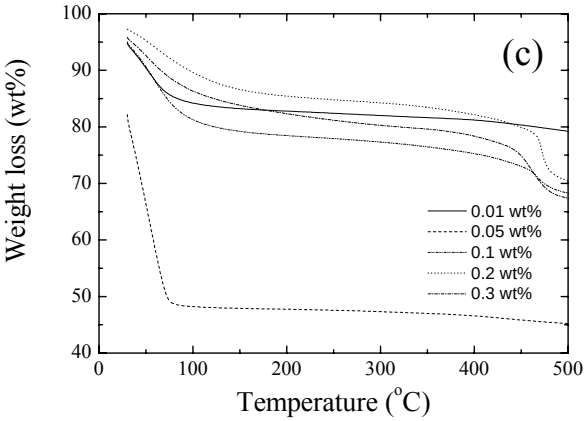

Fig. 9 Weight loss estimated at 25-500°C in different PAA concentrations at different solution pH, (a) pH9, (b) pH10 and (c) pH11